Published in final edited form as:
J Immunol. 2015 January 1; 194(1): 35–42. doi:10.4049/jimmunol.1401158.

ATAD5 Deficiency Decreases B Cell Division and *Igh* Recombination

Kimberly J. Zanotti[*], **Robert W. Maul**[*], **Diana P. Castiblanco**[*], **William Yang**[*], **Yong Jun Choi**[†], **Jennifer T. Fox**[†], **Kyungjae Myung**[†], **Huseyin Saribasak**[*], and **Patricia J. Gearhart**[*]

[*]Laboratory of Molecular Biology and Immunology, National Institute on Aging, National Institutes of Health, Baltimore, MD, 21224

[†]Genetics and Molecular Biology Branch, National Human Genome Research Institute, National Institutes of Health, Bethesda, MD 20892

Abstract

Mammalian ATAD5 and its yeast homolog ELG1 are responsible for unloading PCNA from newly synthesized DNA. Prior work in HeLa and yeast cells showed that a decrease in ATAD5 protein levels resulted in accumulation of chromatin-bound PCNA, slowed cell division and increased genomic instability. In this study, B cells from heterozygous (*Atad5*$^{+/m}$) mice were used to examine the effects of decreased cell proliferation on antibody diversity. ATAD5 haploinsufficiency did not change the frequency or spectrum of somatic hypermutation in antibody genes, indicating that DNA repair and error-prone DNA polymerase η usage were unaffected. However, immunized *Atad5*$^{+/m}$ mice had decreased serum IgG1 antibodies, demonstrating a functional effect on class switch recombination. The mechanism of this altered immune response was then examined following ex vivo stimulation of splenic B cells, where *Atad5*$^{+/m}$ cells accumulated in S phase of the cell cycle and had reduced proliferation compared to wild type cells. These haploinsufficient cells underwent a significant decline in activation-induced deaminase expression, resulting in decreased switch region DNA double-strand breaks and inter-chromosomal translocations in the *Igh* locus. Class switch recombination to several isotypes was also reduced in *Atad5*$^{+/m}$ cells, although the types of end-joining pathways were not affected. These results describe a defect in DNA replication that affects *Igh* recombination via reduced cell division.

Introduction

Following stimulation, B cells express activation-induced deaminase (AID) and undergo rapid division to produce antibodies with improved affinity by somatic hypermutation (SHM) and with different isotypes by class switch recombination (CSR) (1, 2). Thus, cell division following stimulation underpins the swift response of B cells to stimuli. To

Address correspondence and reprint requests either to Dr. Huseyin Saribasak, Sifa University, Ankara Cad. No:45; Bayrakli, Izmir, Turkey, 35100, huseyin.saribasak@sifa.edu.tr. Dr. Patricia J. Gearhart, National Institute on Aging, NIH, 251 Bayview Boulevard, Baltimore, MD, 21224, Phone: (410)-558-8561; Fax: (410)-558-8386; gearhartp@mail.nih.gov.

Disclosures
The authors have no financial conflicts of interest.

understand the effect of DNA replication on SHM and CSR, we studied the role of proliferating cell nuclear antigen (PCNA). PCNA is a sliding clamp protein that forms a homotrimeric ring structure encircling the DNA during replication. Its function is to interact with a plethora of proteins participating in many cellular responses (3), and particularly with DNA polymerases. PCNA holds the replicative polymerases onto the leading and lagging strands to ensure processive synthesis. When damaged bases are encountered, PCNA is mono-ubiquitinated and helps bypass the lesion by exchanging high-fidelity polymerases for low-fidelity ones, such as polymerase (pol) η (4, 5).

In addition to ubiquitination, PCNA is regulated by its loading and unloading from DNA. PCNA needs to be recycled since it binds to the many Okazaki fragments on the lagging strand, and unloading guarantees that enough protein is available for the next round of replication. Although the mechanism of PCNA loading by the replication factor C complex has been studied in detail (6), little is known about how the clamp is unloaded. Recent papers indicate that the yeast enhanced level of genomic instability 1 (ELG1) protein (7, 8) and its mammalian counterpart, ATPase family AAA domain-containing protein 5 (ATAD5) (9), remove PCNA after DNA synthesis (10). In HeLa cells with a knockdown of ATAD5, PCNA accumulated on DNA, which slowed progression of replication forks and cell division (9). In addition, ATAD5 interacts with ubiquitin-specific peptidase 1 at DNA damage bypass sites to de-ubiquitinate PCNA and promote the exchange of a low-fidelity translesion polymerase back to a high-fidelity replication polymerase (11). Thus, ELG1/ATAD5-dependent processing of PCNA is essential for productive DNA replication.

Because ATAD5 is required for embryonic development, heterozygous mice were generated with a mutant allele (*Atad5*$^{+/m}$). These mice are prone to cancers and genomic instability (12). To examine how PCNA manipulation affects the adaptive immune response in B cells, we used *Atad5*$^{+/m}$ mice to study AID-induced SHM and CSR. It is expected that in wild type cells, ATAD5 will successfully unload PCNA from newly synthesized DNA, whereas in *Atad5*$^{+/m}$ cells, PCNA will accumulate on the chromatin (Fig. 1). Amassed PCNA could potentially alter antibody diversity at the *Igh* locus through both prolonged contact of low-fidelity DNA polymerases during SHM and delayed cell division during CSR.

Materials and Methods

Mice

Atad5$^{+/m}$ and *Atad5*$^{+/+}$ mice on a C57BL/6 background were previously described (12). Littermate mice were used at 4-9 months of age. All animal protocols were reviewed and approved by the Animal Care and Use Committees of the National Institute on Aging and the National Human Genome Research Institute.

Splenic B cell isolation and ex vivo stimulation

Resting splenic B cells were collected by negative selection with anti-CD43 and anti-CD11b magnetic beads (Miltenyi Biotec) and cultured in RPMI media (Invitrogen) containing 10% (v/v) fetal bovine serum (Sigma-Aldrich), 100 U/ml penicillin-streptomycin (Invitrogen), 2 mM glutamine (Invitrogen), and 50 μM β-mercaptoethanol (Sigma-Aldrich). Cells were

plated at 0.5×10^6 cells/ml in 24-well plates and stimulated with 5 μg/ml LPS (*E. coli* serotype 0111:B4; Sigma-Aldrich) and 5 ng/ml recombinant interleukin-4 (IL-4) (Biolegend), unless otherwise noted.

Western blot and qPCR

B cells were stimulated for 0-3 days, centrifuged, and suspended in Laemmli lysis buffer. Samples were separated by SDS-PAGE gel electrophoresis using a 4% stacking layer with either an 8% polyacrylamide gel for ATAD5 and β-actin, or a 15% polyacrylamide gel for PCNA and AID. Proteins were transferred to a polyvinylidene difluoride membrane (Biorad) and detected with rabbit anti-ATAD5 (12), mouse anti-β-actin (clone AC-15, Sigma-Aldrich), rabbit anti-PCNA (Abcam), or rabbit anti-AID (13) antibodies with cognate whole molecule anti-horseradish peroxidase (Sigma-Aldrich). Chemiluminescent signals (Pierce ECL Plus Substrate) were quantified in *ImageJ* software. For AID transcript levels, RNA was harvested after 3 d stimulation using an RNeasy Mini Kit (Qiagen). cDNA was reverse-transcribed using RNase H minus M-MLV point mutant (Promega) with oligo(dT) primers (Qiagen), followed by qPCR using iTaq SYBR Green Supermix with ROX (Biorad) with previously published primers (14).

SHM

B cells were obtained either from Peyer's patches of naïve mice or from the spleens of mice immunized with 100 μg NP(30)-CGG (4-hydroxy-3-nitrophenylacetyl hapten, ratio = 30, chicken gamma globulin; Biosearch) in CFA for 2-4 weeks. Germinal center B cells were detected by staining with FITC-labeled anti-B220 (clone RA3-6B2) and Alexafluor647-labeled anti-GL7 (clone GL-7) antibodies (eBioscience). $B220^+GL7^+$ cells were isolated via flow cytometry, and DNA was prepared and amplified by nested PCR using J_H4 intron primers as previously described (15). The PCR products were cloned and sequenced; only unique mutations were counted. Mutation spectra percentages were corrected for base composition of the amplified sequence.

ELISA

Serum was collected by retro-orbital bleeds from mice on days 0 and 14 after immunization with 100 μg NP(30)-CGG in CFA. Wells were sequentially coated with NP(25)-BSA or NP(8)-BSA (Biosearch), 5% BSA (Sigma), serum diluted 1:2500 in BSA, and goat anti-mouse IgG1-HRP (Southern Biotech clonotyping system) diluted 1:1000 in BSA. Antibody expression was detected using a TMB peroxidase substrate kit (Vector Laboratories) and was quantitated on a Biorad Model 680 XR microplate reader.

Cell cycle and division analyses

For cell cycle, B cells were stimulated for 30 hours, followed by fixation in EtOH. Cells were treated with 200 μg/ml RNase A (Sigma-Aldrich), resuspended in 50 μg/ml propidium iodide (Sigma-Aldrich) in PBS, and incubated at 37 °C for 40 min prior to flow cytometry analysis. Cell cycle analysis was performed using a Dean-Jett-Fox model with doublet exclusion in *FlowJo 7.6.5* software. For cell division, B cells were labeled with CFSE (Invitrogen) following the manufacturer's protocol and stimulated for 3 days. Proliferation

was measured by flow cytometry, and the number of cells per generation was calculated using *FlowJo 7.6.5* software. Viability was measured by 7-amino-actinomycin D staining.

Double-strand break detection

DNA was isolated from cells that had been stimulated for 2 days, ligated to a blunt double-strand linker, and amplified by ligation-mediated PCR (LM-PCR) as previously described (16). PCR products were separated by electrophoresis, blotted onto a membrane, and hybridized to a probe located in the switch μ (S_μ) region. Hybridization intensity was quantified using *Image Quant TL* software.

CSR

B cells were stimulated with LPS as described above and with 0.5 μg/ml anti-mouse CD40 (clone FGK45, Enzo Life Sciences). The following cytokines were then added for specific switching: for IgG1, IL-4 as described above; for IgG2b, 2 ng/ml TGF-β (R&D Systems); for IgG3, no additional cytokines; and for IgA, IL-4, TGF-β, and 1.5 ng/mL mouse IL-5 (R&D Systems). Flow cytometry analysis of switched populations was conducted after 4 days using cells stained with FITC- or PerCP-labeled anti-B220 (clone RA3-6B2, eBioscience), and either allophycocyanin-conjugated anti-IgG1 (clone M1-14D12, eBioscience), recombinant PE-conjugated IgG2b, IgG3, or IgA antibodies (Southern Biotech). For germline transcripts, B cells were stimulated 4 days as described above. mRNA was harvested and converted to cDNA as stated for AID qPCR. PCR was performed as given previously (17, 18) using primers synthesized by IDT.

Microhomology and Igh/c-myc translocations

For microhomology, cells were stimulated with LPS for 4 days, and DNA containing S_μ-$S_\gamma 3$ joins was amplified, cloned, and sequenced (19). The nucleotide overlap length was based on perfect homology with no insertions. For translocations, cells were stimulated with LPS and IL-4, and harvested after 3 days. *Igh/c-myc* translocations were detected on chromosomes 12 or 15 using nested PCR analysis as previously described (20, 21) with 10^5 cells per PCR amplification. PCR products were separated by gel electrophoresis, blotted and probed sequentially with *Igh*- and *c-myc*-specific oligonucleotides.

Results

Atad5$^{+/m}$ *B cells have decreased ATAD5 expression*

To confirm that heterozygous mice had down-regulated ATAD5, splenic B cells were stimulated ex vivo with LPS and IL-4, and protein expression was measured over time. ATAD5 was not observed in total cell extracts prior to stimulation, but was detected as the cells began to enter S phase at d 1 (Fig. 2A). ATAD5 levels continued to increase at d 2 and plateaued by d 3. ATAD5 down-regulation in heterozygous cells was readily apparent 1 day after stimulation, with a significant 56% reduction in protein levels compared to wild type (Fig. 2B). PCNA levels were likewise measured in cell extracts to test if ATAD5 deficiency affects PCNA expression. As with ATAD5, PCNA upregulation occurred upon B cell entry into S phase (Fig. 2A). There was no significant difference in PCNA expression in *Atad5*$^{+/m}$ cells relative to wild type (Fig. 2C), which is similar to a report that deletion of ELG1 in

yeast had no effect on PCNA levels (7). Thus, *Atad5*$^{+/m}$ cells express less cognate protein after stimulation but still maintain normal PCNA levels, indicating that the heterozygous mice are an appropriate model to study the effect of ATAD5 deficiency on B cell responses.

Atad5$^{+/m}$ mice have unaltered SHM and decreased serum IgG1 in vivo

ATAD5 regulates the access of the low-fidelity pol η to DNA through mono-ubiquitinated PCNA (11, 22), and a deficiency in pol η results in reduced mutations of A and T bases during SHM (15, 23-25). If pol η activity was altered in *Atad5*$^{+/m}$ cells, mutations at A:T bp would be changed. To test this, SHM was examined in a 492-bp region spanning the intron downstream of the rearranged J_H4 gene segment in the *Igh* locus. Germinal center B cells were isolated from either chronically stimulated Peyer's patches in 4 or 9 month old mice (Fig. 3A), or spleens from mice 14 or 28 days after immunization with NP-CGG (Fig. 3B). In Peyer's patch cells, mutation frequencies were similar in mice from both genotypes, and increased with age in accord with previous studies (16, 26). In immunized spleen cells, the frequencies were also similar between genotypes, and did not significantly change between days 14 and 28. Importantly, there was no difference in the spectra of mutations, particularly mutations of A and T bases, in *Atad5*$^{+/m}$ cells compared to wild type cells from both Peyer's patches and immunized spleens. These results indicate that ATAD5 haploinsufficiency did not alter DNA repair (no change in mutation frequency) or DNA polymerase η usage (no change in A:T mutations).

However, a significant impairment in IgG1 antibody production occurred in *Atad5*$^{+/m}$ mice. Mice were immunized with NP-CGG, and serum IgG1 levels were measured by ELISA on days 0 and 14. The average antibody affinity was determined using different conjugates of NP-conjugated BSA on microtiter plates. Both high- and low-affinity antibodies bind to high density NP(25) antigen, but only high-affinity antibody binds to low density NP(8) antigen. At 14 days post-immunization, *Atad5*$^{+/m}$ mice exhibited a significant 22% decrease in total NP-specific antibody binding to NP(25) conjugates relative to wild type mice (Fig 3C). There was no difference in the amount of high-affinity antibody binding to NP(8) conjugates (Fig. 3D), or in the ratio of antibody binding to NP(8) and NP(25) (Fig. 3E). These in vivo studies indicate that ATAD5 deficiency negatively affects IgG1 antibody production, but does not impact SHM or affinity maturation.

Atad5$^{+/m}$ cells accumulate in S phase and have decreased proliferation

To probe the mechanism behind reduced IgG1 serum antibody in *Atad5*$^{+/m}$ mice, we examined CSR in cells synchronously stimulated ex vivo with LPS and IL-4. Prior work has shown that small interfering RNA knockdown of ATAD5 in HeLa cells (9) and depletion of ELG1 protein in yeast cells (7) resulted in a delayed S phase. It has been proposed that decreased ATAD5 levels inhibit the unloading of PCNA at replication forks, and these cells are unable to progress through cell division until PCNA is unloaded post-replication. Thus, cells pile up in S phase of the cell cycle and DNA replication is slowed. To test whether a similar effect occurred in *Atad5* heterozygous mice, the number of cells in G_1, S, or G_2 phases was measured. Stimulated B cells, which initially enter S phase at 24 hours, were collected at 30 hours. Cells were fixed with EtOH and stained with propidium iodide to measure cell cycle phase. A significant number of *Atad5*$^{+/m}$ cells accumulated in S phase

relative to wild type (Fig. 4A). No significant changes were apparent in the number of cells in G_1, when AID and UNG create breaks for CSR (27, 28), or G_2.

The increased number of cells in S phase may correlate with decreased cell division. Cell division was tested via CFSE-labeling prior to ex vivo stimulation. At 3 d, cells were analyzed by flow cytometry (Fig. 4B) and the number of cells per generation was calculated (Fig. 4C). There was a significant difference between the two genotypes, with a greater percentage of *Atad5*$^{+/m}$ cells in generations 3 and 4, while a higher percentage of wild type cells was present in generation 5, signifying that the haploinsufficient cells had slower cell division. This was not due to increased apoptosis, as cell viability was not affected by *Atad5* heterozygosity during the stimulation period (data not shown). The cell cycle and division data indicate that ATAD5 aids in the progression of B cells through S phase during cell division.

Since levels of AID protein have been shown to increase with successive cell divisions (29), AID expression was measured by both qPCR of mRNA transcripts and Western blot of protein in *Atad5*$^{+/m}$ B cells after 3 days of stimulation. The amount of AID mRNA and protein was significantly lower in the heterozygous cells (Fig. 4D), likely due to their decreased proliferation. It is thus probable that these cells will be impaired for CSR.

Atad5$^{+/m}$ cells have reduced double-strand breaks, CSR, and translocations

RNA polymerase II accumulates in the S_μ region of DNA (30, 31) and interacts with cofactors to recruit AID protein (32, 33). AID then deaminates cytosine to uracil (34), and uracils are processed into double-strand breaks, which serve as substrates for CSR and translocations. We therefore tested if the decreased proliferation of *Atad5*$^{+/m}$ cells leads to reduced recombination in S_μ. Recombination in ex vivo stimulated B cells was examined at multiple levels: double-strand break formation, CSR, and *Igh* translocation to the *c-myc* locus.

To measure double-strand breaks, an oligonucleotide linker was ligated to genomic DNA from cells after 2 days of stimulation. The samples were then amplified by LM-PCR (Fig. 5A) (16, 35, 36), separated by gel electrophoresis, and the products containing S_μ DNA were identified by hybridization (Fig. 5B). When the hybridization intensity was quantified, *Atad5*$^{+/m}$ cells possessed a significant decrease in breaks compared to *Atad5*$^{+/+}$ cells (Fig. 5C).

The reduction in double-strand breaks will likely decrease CSR. A significant average decline of 37% in IgG1 switching relative to wild type occurred in *Atad5*$^{+/m}$ cells stimulated ex vivo with LPS, anti-CD40, and IL-4 (Fig. 6A), similar to the decrease in serum IgG1 14 days after immunization. To test if switching to other isotypes was also decreased, we activated cells under different conditions. There were significant declines of 34% and 29% relative to wild type respectively for IgG2b and IgA, and a modest decrease in IgG3. It is possible that the decreased CSR is caused by insufficient germline transcription of acceptor switch regions to promote AID binding. Transcript levels following stimulation were measured for γ1, γ2b, γ3, and α regions, but there was no change relative to wild type (data

not shown). This suggests that the decline in *Atad5*$^{+/m}$ CSR is not due to reduced access of AID to acceptor switch regions.

CSR can also be affected by the type of non-homologous end joining using either the classical or alternate pathways, which is determined by the microhomology length of the joined products. Classical end-joining is characterized by blunt or short overlapping sequences, whereas alternate end-joining uses longer overlaps (37, 38). Lengths of joins were measured in B cells stimulated with LPS for 4 days to induce switching to IgG3. $S_\gamma 3$ was chosen because it is shorter than other S regions, which makes it easier to identify homology after recombination. DNA containing S_μ-$S_\gamma 3$ joins was amplified, sequenced, and analyzed for the number of identical bases, or microhomology, shared between S_μ and $S_\gamma 3$ at the break site. There was no difference in the mean length in *Atad5*$^{+/m}$ cells (1.5 bp) compared with *Atad5*$^{+/+}$ cells (1.3 bp) (Fig. 6B), suggesting that the decline in CSR was not due to changes in end joining.

Double-strand breaks can instigate translocations between S_μ on chromosome 12 and exon 1 of the *c-myc* gene on chromosome 15. After 2 days in culture, translocations were measured using primers to amplify the recombined loci (Fig. 7A), and products were separated by gel electrophoresis and identified by Southern hybridization with both *Igh* and *c-myc* probes (Fig. 7B). An analysis of ~350 independent amplification reactions per genotype showed that *Atad5*$^{+/m}$ cells had signficantly reduced levels of translocations, with 2.1 translocations per 10^7 cells, compared to wild type cells, with 4.6 translocations per 10^7 cells (Fig. 7C). These results indicate that fewer double-strand breaks in short-term cultures of *Atad5*$^{+/m}$ primary cells correlated with fewer translocations. Taken together, the data show that ATAD5's role in DNA replication substantially restricted AID activity in recombination at the *Igh* locus.

Discussion

Upon activation, B cells undergo rapid expansion through several rounds of DNA replication and cell division, triggering AID-induced modification of antibody genes on the *Igh* locus. Previous work has shown that there is a tight correlation between cell proliferation, AID expression, and CSR (29, 36, 39, 40); however, the role of DNA replication in promoting SHM and CSR has not been fully examined. In this report, we focused on the ATAD5 protein, which is required for unloading the PCNA clamp at the DNA replication fork. Aberrant unloading could have two consequences on antibody diversity. First, prolonged contact of the clamp with the low-fidelity pol η could affect SHM frequencies and mutation spectra. Second, retention of the clamp could affect CSR by slowing DNA replication and subsequent cell division. We used an *Atad5*$^{+/m}$ mouse model with defective DNA replication to demonstrate that a delay in cell cycle slows cell division and decreases *Igh* recombination.

Concerning SHM, although AID generates uracils during the G_1 cell cycle phase (27), fixation of uracils into permanent mutations occurs during DNA replication across the mutation site in S phase. The SHM frequency and spectra in the J_H4 intronic region were measured in germinal center cells from chronically stimulated Peyer's patches and from

immunized spleens. There was no statistical difference in mutation frequencies between *Atad5*$^{+/+}$ and *Atad5*$^{+/m}$ cells in either case, suggesting that ATAD5 haploinsufficiency and accumulation of cells in S phase did not alter fixation of uracils and their subsequent repair. In addition to releasing unmodified PCNA at replication forks, ATAD5 has been shown to regulate the levels of mono-ubiquitinated PCNA after DNA damage (11). Because pol η is dependent upon PCNA mono-ubiquitination during SHM, we looked for a change in mutations at A and T bases (25, 41). Surprisingly, there were no alterations to the mutational spectra in either Peyer's patch or immunized spleen cells, suggesting proper pol η function during SHM. Thus, decreased levels of the PCNA handler, ATAD5, did not affect SHM.

Concerning CSR, PCNA accumulation did impair switching in vivo, as evidenced by significantly reduced serum IgG1 antibodies in *Atad5*$^{+/m}$ mice 14 days post-immunization. There was no change in affinity maturation in the heterozygous serum pool compared to wild type, indicating that selection for affinity was unaffected, which is consistent with the similar SHM frequencies. The cellular processes responsible for reduced switching were examined in more detail in ex vivo studies, where cells could be synchronously stimulated. Compared to wild type cells, *Atad5*$^{+/m}$ cells exhibited a build-up in S phase that led to significantly decreased proliferation. CSR is known to be linked to the number of cell divisions (42, 43) through increased AID expression (29). In agreement with these reports, the delayed cell division observed in *Atad5*$^{+/m}$ cells corresponded with a decrease in AID expression. This reduced the amount of double-strand breaks in the S_{μ} region, which act as the initiating lesions for recombination. Inter-chromosomal recombinations between S_{μ} and *c-myc* were likewise decreased. The frequency of CSR to several isotypes was also diminished, which might be due to different usage of the two pathways regulating non-homologous end joining. Classical, or blunt, end-joining yields predominantly productive recombination between two switch regions, resulting in CSR. Alternative, or microhomology-mediated, end-joining is associated with intra-switch recombination within a S region, producing no CSR (44, 45). The decrease in CSR and translocations does not appear to be due to defects in non-homologous recombination pathways, since there was no difference in microhomology lengths between *Atad5*$^{+/m}$ and wild type cells. Rather, decreased proliferation lowered AID production, which then diminished strand breaks and yielded fewer recombination events. Our results are similar to the diminished CSR in mice haploinsufficient for AID (46), but emphasize that delayed division, which also decreases AID, compromises *Igh* recombination as well. In total, our data suggest that ATAD5 deficiency indirectly regulates AID expression and CSR through delayed DNA replication.

Numerous proteins affect CSR through the mechanics of break recognition and joining (Ku70/80, DNA-PKcs, XRCC4, Lig4), chromatin-associated complexes at double-strand breaks (ATM, H2AX, MDC1, cohesin), and break processing (53BP1, Mre11, CtIP value, Rad9, RecQ helicases, Exo1, mismatch repair proteins, DNA polymerase ζ) (47-53). Mice with genetic defects in these proteins often have complicated phenotypes which simultaneously change multiple components of CSR. Therefore, it becomes difficult to ascertain the specific role of DNA replication in isotype switching. The experiments presented here demonstrate that a mutation that delays completion of DNA replication and

cell division alters the immune response by reducing AID-dependent double-strand breaks and CSR.

Acknowledgments

We thank Zheng Cao for technical support; R. Wersto, J. Scheers, C. Nguyen, and T. Wallace of the NIA flow cytometry unit for sorting; and Robert Brosh and Ranjan Sen for insightful comments.

This research was supported entirely by the Intramural Research Program of the NIH: National Institute on Aging, National Human Genome Research Institute, and AIDS Intramural Research Fellowship (D.P.C.). D.P.C. is in the Immunology Training Program at the Johns Hopkins University School of Medicine.

Abbreviations

AID	activation-induced deaminase
ATAD5	ATPase family AAA domain-containing protein 5
CSR	class switch recombination
ELG1	enhanced level of genomic instability 1
LM-PCR	ligation mediated-PCR
PCNA	proliferating cell nuclear antigen
SHM	somatic hypermutation

References

1. Maul RW, Gearhart PJ. AID and somatic hypermutation. Adv Immunol. 2010; 105:159–191. [PubMed: 20510733]
2. Stavnezer J, Guikema JE, Schrader CE. Mechanism and regulation of class switch recombination. Annu Rev Immunol. 2008; 26:261–292. [PubMed: 18370922]
3. Moldovan GL, Pfander B, Jentsch S. PCNA, the maestro of the replication fork. Cell. 2007; 129:665–679. [PubMed: 17512402]
4. Kannouche PL, Wing J, Lehmann AR. Interaction of human DNA polymerase eta with monoubiquitinated PCNA: a possible mechanism for the polymerase switch in response to DNA damage. Mol Cell. 2004; 14:491–500. [PubMed: 15149598]
5. Garg P, Burgers PM. Ubiquitinated proliferating cell nuclear antigen activates translesion DNA polymerases eta and REV1. Proc Natl Acad Sci USA. 2005; 102:18361–18366. [PubMed: 16344468]
6. Hedglin M, Kumar R, Benkovic SJ. Replication clamps and clamp loaders. Cold Spring Harbor Perspectives in Biology. 2013; 5 a010165.
7. Kubota T, Nishimura K, Kanemaki MT, Donaldson AD. The Elg1 replication factor C-like complex functions in PCNA unloading during DNA replication. Mol Cell. 2013; 50:273–280. [PubMed: 23499004]
8. Shiomi Y, Nishitani H. Alternative replication factor C protein, Elg1, maintains chromosome stability by regulating PCNA levels on chromatin. Genes Cells. 2013; 18:946–959. [PubMed: 23937667]
9. Lee KY, Fu H, Aladjem MI, Myung K. ATAD5 regulates the lifespan of DNA replication factories by modulating PCNA level on the chromatin. J Cell Biol. 2013; 200:31–44. [PubMed: 23277426]
10. Ulrich HD. New insights into replication clamp unloading. J Mol Biol. 2013; 425:4727–4732. [PubMed: 23688817]

11. Lee KY, Yang K, Cohn M, Sikdar N, D'Andrea A, Myung K. Human ELG1 regulates the level of ubiquitinated proliferating cell nuclear antigen (PCNA) through its interactions with PCNA and USP1. J Biol Chem. 2010; 285:10362–10369. [PubMed: 20147293]
12. Bell DW, Sikdar N, Lee KY, Price JC, Chatterjee R, Park HD, Fox J, Ishiai M, Rudd ML, Pollock LM, Fogoros SK, Mohamed H, Hanigan CL, Program NCS, Zhang S, Cruz P, Renaud G, Hansen NF, Cherukuri PF, Borate B, McManus KJ, Stoepel J, Sipahimalani P, Godwin AK, Sgroi DC, Merino MJ, Elliot G, Elkahloun A, Vinson C, Takata M, Mullikin JC, Wolfsberg TG, Hieter P, Lim DS, Myung K. Predisposition to cancer caused by genetic and functional defects of mammalian Atad5. PLoS Genet. 2011; 7:e1002245. [PubMed: 21901109]
13. Kohli RM, Maul RW, Guminski AF, McClure RL, Gajula KS, Saribasak H, McMahon MA, Siliciano RF, Gearhart PJ, Stivers JT. Local sequence targeting in the AID/APOBEC family differentially impacts retroviral restriction and antibody diversification. J Biol Chem. 2010; 285:40956–40964. [PubMed: 20929867]
14. Maul RW, Cao Z, Venkataraman L, Giorgetti CA, Press JL, Denizot Y, Du H, Sen R, Gearhart PJ. Spt5 accumulation at variable genes distinguishes somatic hypermutation in germinal center B cells from ex vivo-activated cells. J Exp Med. 2014; 211:2297–2306. [PubMed: 25288395]
15. Martomo SA, Yang WW, Wersto RP, Ohkumo T, Kondo Y, Yokoi M, Masutani C, Hanaoka F, Gearhart PJ. Different mutation signatures in DNA polymerase eta- and MSH6-deficient mice suggest separate roles in antibody diversification. Proc Natl Acad Sci USA. 2005; 102:8656–8661. [PubMed: 15939880]
16. Saribasak H, Maul RW, Cao Z, McClure RL, Yang W, McNeill DR, Wilson DM 3rd, Gearhart PJ. XRCC1 suppresses somatic hypermutation and promotes alternative nonhomologous end joining in Igh genes. J Exp Med. 2011; 208:2209–2216. [PubMed: 21967769]
17. Park SR, Seo GY, Choi AJ, Stavnezer J, Kim PH. Analysis of transforming growth factor-beta1-induced Ig germ-line gamma2b transcription and its implication for IgA isotype switching. Eur J Immunol. 2005; 35:946–956. [PubMed: 15688346]
18. Fang CM, Roy S, Nielsen E, Paul M, Maul R, Paun A, Koentgen F, Raval FM, Szomolanyi-Tsuda E, Pitha PM. Unique contribution of IRF-5-Ikaros axis to the B-cell IgG2a response. Genes Immun. 2012; 13:421–430. [PubMed: 22535200]
19. Wu X, Stavnezer J. DNA polymerase beta is able to repair breaks in switch regions and plays an inhibitory role during immunoglobulin class switch recombination. J Exp Med. 2007; 204:1677–1689. [PubMed: 17591858]
20. Ramiro AR, Jankovic M, Eisenreich T, Difilippantonio S, Chen-Kiang S, Muramatsu M, Honjo T, Nussenzweig A, Nussenzweig MC. AID is required for c-myc/IgH chromosome translocations in vivo. Cell. 2004; 118:431–438. [PubMed: 15315756]
21. Ramiro AR, Jankovic M, Callen E, Difilippantonio S, Chen HT, McBride KM, Eisenreich TR, Chen J, Dickins RA, Lowe SW, Nussenzweig A, Nussenzweig MC. Role of genomic instability and p53 in AID-induced c-myc-Igh translocations. Nature. 2006; 440:105–109. [PubMed: 16400328]
22. Bienko M, Green CM, Sabbioneda S, Crosetto N, Matic I, Hibbert RG, Begovic T, Niimi A, Mann M, Lehmann AR, Dikic I. Regulation of translesion synthesis DNA polymerase eta by monoubiquitination. Mol Cell. 2010; 37:396–407. [PubMed: 20159558]
23. Zeng X, Winter DB, Kasmer C, Kraemer KH, Lehmann AR, Gearhart PJ. DNA polymerase eta is an A-T mutator in somatic hypermutation of immunoglobulin variable genes. Nat Immunol. 2001; 2:537–541. [PubMed: 11376341]
24. Delbos F, De Smet A, Faili A, Aoufouchi S, Weill JC, Reynaud CA. Contribution of DNA polymerase eta to immunoglobulin gene hypermutation in the mouse. J Exp Med. 2005; 201:1191–1196. [PubMed: 15824086]
25. Langerak P, Nygren AO, Krijger PH, van den Berk PC, Jacobs H. A/T mutagenesis in hypermutated immunoglobulin genes strongly depends on PCNAK164 modification. J Exp Med. 2007; 204:1989–1998. [PubMed: 17664295]
26. Gonzalez-Fernandez A, Gilmore D, Milstein C. Age-related decrease in the proportion of germinal center B cells from mouse Peyer's patches is accompanied by an accumulation of somatic mutations in their immunoglobulin genes. Eur J Immunol. 1994; 24:2918–2921. [PubMed: 7957583]

27. Schrader CE, Guikema JE, Linehan EK, Selsing E, Stavnezer J. Activation-induced cytidine deaminase-dependent DNA breaks in class switch recombination occur during G1 phase of the cell cycle and depend upon mismatch repair. J Immunol. 2007; 179:6064–6071. [PubMed: 17947680]

28. Sharbeen G, Yee CW, Smith AL, Jolly CJ. Ectopic restriction of DNA repair reveals that UNG2 excises AID-induced uracils predominantly or exclusively during G1 phase. J Exp Med. 2012; 209:965–974. [PubMed: 22529268]

29. Rush J, Liu M, Odegard V, Unniraman S, Schatz D. Expression of activation-induced cytidine deaminase is regulated by cell division, providing a mechanistic basis for division-linked class switch recombination. Proc Natl Acad Sci USA. 2005; 102:13242–13247. [PubMed: 16141332]

30. Rajagopal D, Maul RW, Ghosh A, Chakraborty T, Khamlichi AA, Sen R, Gearhart PJ. Immunoglobulin switch mu sequence causes RNA polymerase II accumulation and reduces dA hypermutation. J Exp Med. 2009; 206:1237–1244. [PubMed: 19433618]

31. Wang L, Wuerffel R, Feldman S, Khamlichi AA, Kenter AL. S region sequence, RNA polymerase II, and histone modifications create chromatin accessibility during class switch recombination. J Exp Med. 2009; 206:1817–1830. [PubMed: 19596805]

32. Pavri R, Gazumyan A, Jankovic M, Di Virgilio M, Klein I, Ansarah-Sobrinho C, Resch W, Yamane A, Reina San-Martin B, Barreto V, Nieland TJ, Root DE, Casellas R, Nussenzweig MC. Activation-induced cytidine deaminase targets DNA at sites of RNA polymerase II stalling by interaction with Spt5. Cell. 2010; 143:122–133. [PubMed: 20887897]

33. Basu U, Meng FL, Keim C, Grinstein V, Pefanis E, Eccleston J, Zhang T, Myers D, Wasserman CR, Wesemann DR, Januszyk K, Gregory RI, Deng H, Lima CD, Alt FW. The RNA exosome targets the AID cytidine deaminase to both strands of transcribed duplex DNA substrates. Cell. 2011; 144:353–363. [PubMed: 21255825]

34. Petersen-Mahrt SK, Harris RS, Neuberger MS. AID mutates E. coli suggesting a DNA deamination mechanism for antibody diversification. Nature. 2002; 418:99–103. [PubMed: 12097915]

35. Wuerffel R, Du J, Thompson R, Kenter AL. Ig Sγ3 DNA-specific double strand breaks are induced in mitogen-activated B cells and are implicated in switch recombination. J Immunol. 1997; 159:4139–4144. [PubMed: 9379005]

36. Schrader CE, Linehan EK, Mochegova SN, Woodland RT, Stavnezer J. Inducible DNA breaks in Ig S regions are dependent on AID and UNG. J Exp Med. 2005; 202:561–568. [PubMed: 16103411]

37. Yan CT, Boboila C, Souza EK, Franco S, Hickernell TR, Murphy M, Gumaste S, Geyer M, Zarrin AA, Manis JP, Rajewsky K, Alt FW. IgH class switching and translocations use a robust non-classical end-joining pathway. Nature. 2007; 449:478–482. [PubMed: 17713479]

38. Pan-Hammarstrom Q, Jones AM, Lahdesmaki A, Zhou W, Gatti RA, Hammarstrom L, Gennery AR, Ehrenstein MR. Impact of DNA ligase IV on nonhomologous end joining pathways during class switch recombination in human cells. J Exp Med. 2005; 201:189–194. [PubMed: 15657289]

39. Heltemes-Harris LM, Gearhart PJ, Ghosh P, Longo DL. Activation-induced deaminase-mediated class switch recombination is blocked by anti-IgM signaling in a phosphatidylinositol 3-kinase-dependent fashion. Mol Immunol. 2008; 45:1799–1806. [PubMed: 17983655]

40. Maul RW, Saribasak H, Martomo SA, McClure RL, Yang W, Vaisman A, Gramlich HS, Schatz DG, Woodgate R, Wilson DM 3rd, Gearhart PJ. Uracil residues dependent on the deaminase AID in immunoglobulin gene variable and switch regions. Nat Immunol. 2011; 12:70–76. [PubMed: 21151102]

41. Roa S, Avdievich E, Peled JU, Maccarthy T, Werling U, Kuang FL, Kan R, Zhao C, Bergman A, Cohen PE, Edelmann W, Scharff MD. Ubiquitylated PCNA plays a role in somatic hypermutation and class-switch recombination and is required for meiotic progression. Proc Natl Acad Sci USA. 2008; 105:16248–16253. [PubMed: 18854411]

42. Hodgkin PD, Lee JH, Lyons AB. B cell differentiation and isotype switching is related to division cycle number. J Exp Med. 1996; 184:277–281. [PubMed: 8691143]

43. Hasbold J, Lyons AB, Kehry MR, Hodgkin PD. Cell division number regulates IgG1 and IgE switching of B cells following stimulation by CD40 ligand and IL-4. Eur J Immunol. 1998; 28:1040–1051. [PubMed: 9541600]

44. Zarrin AA, Del Vecchio C, Tseng E, Gleason M, Zarin P, Tian M, Alt FW. Antibody class switching mediated by yeast endonuclease-generated DNA breaks. Science. 2007; 315:377–381. [PubMed: 17170253]
45. Bothmer A, Robbiani DF, Feldhahn N, Gazumyan A, Nussenzweig A, Nussenzweig MC. 53BP1 regulates DNA resection and the choice between classical and alternative end joining during class switch recombination. J Exp Med. 2010; 207:855–865. [PubMed: 20368578]
46. Takizawa M, Tolarova H, Li Z, Dubois W, Lim S, Callen E, Franco S, Mosaico M, Feigenbaum L, Alt FW, Nussenzweig A, Potter M, Casellas R. AID expression levels determine the extent of cMyc oncogenic translocations and the incidence of B cell tumor development. J Exp Med. 2008; 205:1949–1957. [PubMed: 18678733]
47. Stavnezer J, Bjorkman A, Du L, Cagigi A, Pan-Hammarstrom Q. Mapping of switch recombination junctions, a tool for studying DNA repair pathways during immunoglobulin class switching. Adv Immunol. 2010; 108:45–109. [PubMed: 21056729]
48. Lieber MR. The mechanism of double-strand DNA break repair by the nonhomologous DNA end-joining pathway. Annu Rev Biochem. 2010; 79:181–211. [PubMed: 20192759]
49. Boboila C, Alt FW, Schwer B. Classical and alternative end-joining pathways for repair of lymphocyte-specific and general DNA double-strand breaks. Adv Immunol. 2012; 116:1–49. [PubMed: 23063072]
50. Bothmer A, Rommel PC, Gazumyan A, Polato F, Reczek CR, Muellenbeck MF, Schaetzlein S, Edelmann W, Chen PL, Brosh RM Jr. Casellas R, Ludwig T, Baer R, Nussenzweig A, Nussenzweig MC, Robbiani DF. Mechanism of DNA resection during intrachromosomal recombination and immunoglobulin class switching. J Exp Med. 2013; 210:115–123. [PubMed: 23254285]
51. An L, Wang Y, Liu Y, Yang X, Liu C, Hu Z, He W, Song W, Hang H. Rad9 is required for B cell proliferation and immunoglobulin class switch recombination. J Biol Chem. 2010; 285:35267–35273. [PubMed: 20729201]
52. Thomas-Claudepierre AS, Schiavo E, Heyer V, Fournier M, Page A, Robert I, Reina-San-Martin B. The cohesin complex regulates immunoglobulin class switch recombination. J Exp Med. 2013; 210:2495–2502. [PubMed: 24145512]
53. Enervald E, L Du, Visnes T, Bjorkman A, Lindgren E, Wincent J, Borck G, Colleaux L, Cormier-Daire V, van Gent DC, Pie J, Puisac B, de Miranda NF, Kracker S, Hammarstrom L, de Villartay JP, Durandy A, Schoumans J, Strom L, Pan-Hammarstrom Q. A regulatory role for the cohesin loader NIPBL in nonhomologous end joining during immunoglobulin class switch recombination. J Exp Med. 2013; 210:2503–2513. [PubMed: 24145515]

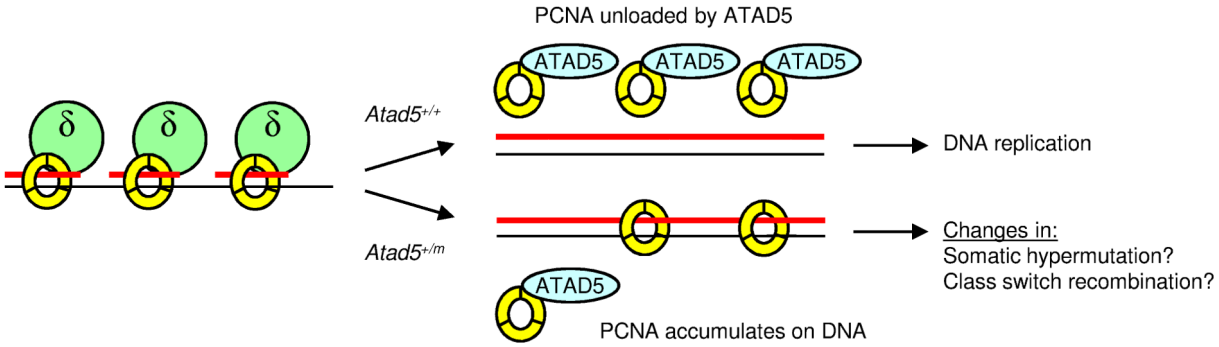

FIGURE 1.

Model for DNA replication. Homotrimeric PCNA (yellow ring) binds to Okazaki fragments (short red lines) and holds the high-fidelity DNA polymerase δ (green circle) on the template DNA. In wild type cells, ATAD5 (blue oval) unloads PCNA from the replication fork after DNA synthesis is complete. In *Atad5*$^{+/m}$ cells, PCNA accumulates on the chromatin and may affect the immune response.

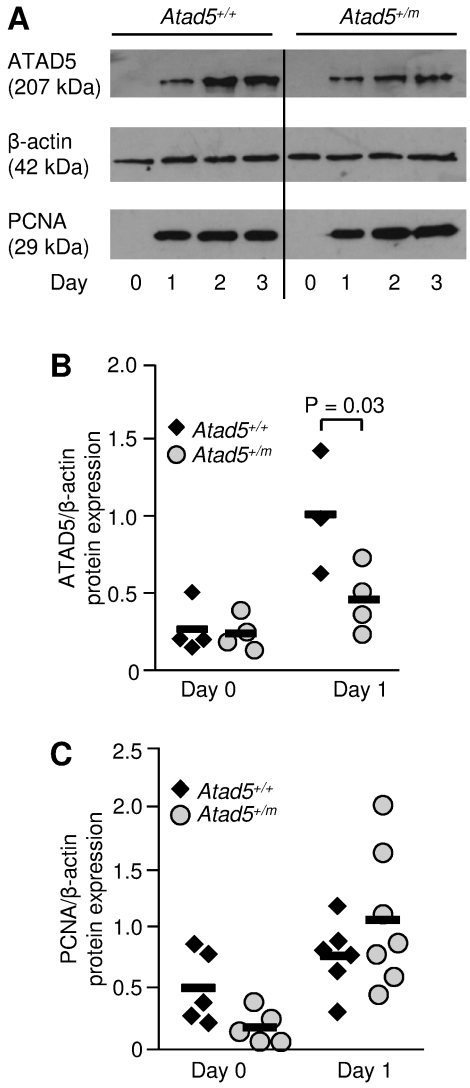

FIGURE 2.

ATAD5 down-regulation in heterozygous B cells. **(A)** ATAD5, β-actin, and PCNA protein levels in *Atad5*$^{+/+}$ and *Atad5*$^{+/m}$ cells. Representative Western blot analysis of splenic B cells stimulated with LPS and IL-4 for 0-3 days. **(B)** Quantification of Western blot signal for ATAD5 normalized to β-actin for cells from wild type (diamond) or heterozygous (circle) mice stimulated for 0 or 1 day. Bars indicate average signal. Data are from 3-4 mice per genotype using one mouse per experiment. P value, one-tailed equal variance Student's *t*-test. **(C)** Western blot signal for PCNA normalized to β-actin, similar to (B). Data are from 5-7 mice of each genotype with one mouse per experiment.

A Mutations in J_H4 region from Peyer's patch B cells

	4 month old		9 month old	
	Atad5$^{+/+}$	*Atad5*$^{+/m}$	*Atad5*$^{+/+}$	*Atad5*$^{+/m}$
Number of sequences	76	150	117	94
Mutated sequences	30	61	58	39
Bases in mutated sequences	14,760	30,012	28,536	19,188
Mutations	147	382	601	343
Mutations/base in mutated sequences	1.0×10^{-2}	1.3×10^{-2}	2.1×10^{-2}	1.8×10^{-2}

Mutation spectra percentages for Peyer's patch cells

Atad5$^{+/+}$ (748 mutations)

From \ To	A	T	G	C	Total
A	-	10	16	8	34
T	5	-	5	10	20
G	12	3	-	6	21
C	6	15	4	-	25

Atad5$^{+/m}$ (725 mutations)

From \ To	A	T	G	C	Total
A	-	9	16	7	32
T	5	-	4	10	19
G	14	5	-	6	25
C	5	14	5	-	24

B Mutations in J_H4 region from immunized splenic B cells

	14 days		28 days	
	Atad5$^{+/+}$	*Atad5*$^{+/m}$	*Atad5*$^{+/+}$	*Atad5*$^{+/m}$
Number of sequences	346	288	130	103
Mutated sequences	53	77	26	32
Bases in mutated sequences	26,076	37,884	12,792	15,744
Mutations	161	263	100	107
Mutations/base in mutated sequences	6.2×10^{-3}	6.9×10^{-3}	7.8×10^{-3}	6.8×10^{-3}

Mutation spectra percentages for immunized spleen cells

Atad5$^{+/+}$ (261 mutations)

From \ To	A	T	G	C	Total
A	-	7	17	6	30
T	6	-	3	10	19
G	14	4	-	8	26
C	5	15	5	-	25

Atad5$^{+/m}$ (370 mutations)

From \ To	A	T	G	C	Total
A	-	9	13	5	27
T	6	-	4	10	20
G	10	3	-	10	23
C	7	19	4	-	30

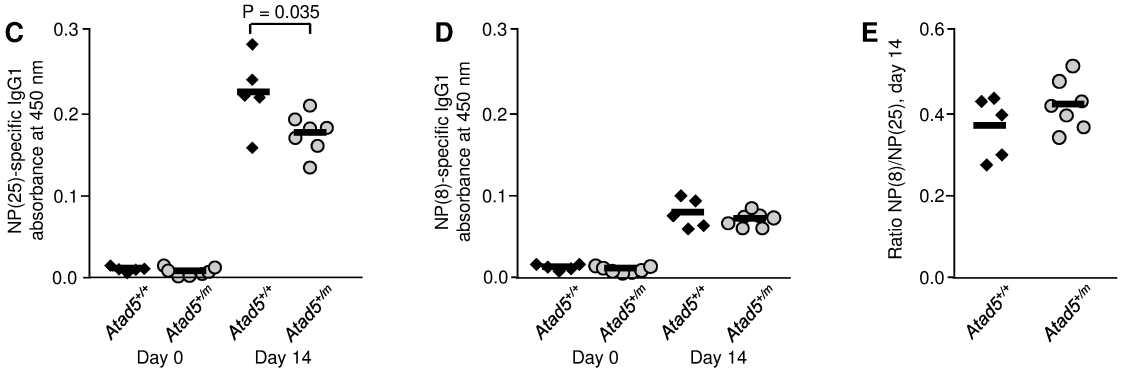

FIGURE 3.

Effect of ATAD5 down-regulation on SHM and CSR in mice. **(A)** SHM frequency and spectra in Peyer's patch germinal center B cells from 4 and 9 month old mice. Data are from 4-5 independent experiments each using 2-3 mice per genotype. **(B)** SHM frequency and spectra in splenic germinal center B cells 14 and 28 days after immunization with NP-CGG. Data are from 4 independent experiments with 5-7 mice per genotype. **(C-E)** Serum NP-specific IgG1 expression measured by ELISA after immunization. Bars indicate average signal. Data are from 6 independent experiments with 5-7 mice per genotype, using one mouse per experiment. (C) High- and low-affinity antibodies bound to NP(25)-BSA. P value, two-tailed equal variance Student's *t*-test. (D) High-affinity antibody bound to NP(8)-BSA. (E) Ratio of NP(8) binding to NP(25) binding.

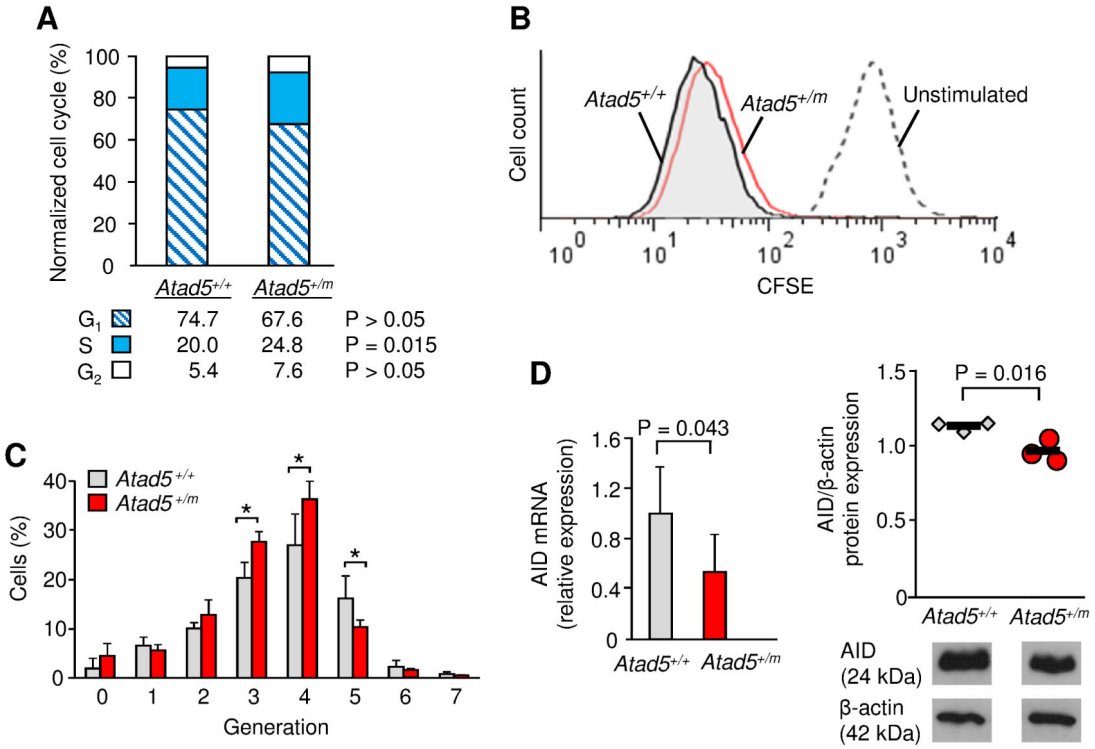

FIGURE 4.

Cell cycle, proliferation, and AID analyses. **(A)** Percent of cells in cell cycle phases after 30 h of stimulation. Data were averaged from 3 experiments with one mouse per genotype per experiment. P value, two-tailed paired Student's *t*-test. **(B)** Representative CFSE labeling histogram from cells prior to stimulation (dashed line), or post-stimulation wild type (shaded black line) or *Atad5*$^{+/m}$ (red line) cells. **(C)** Quantification of CFSE-labeled cells. Error bars signify the SD of values from 5 independent experiments with one mouse per genotype. Asterisks indicate significance with $P < 0.05$; two-tailed equal variance Student's *t*-test. **(D)** AID expression in *Atad5*$^{+/+}$ or *Atad5*$^{+/m}$ B cells after 3 d stimulation. AID mRNA transcript levels were measured by qPCR and normalized to β-actin. P value, one-tailed equal variance Student's *t*-test. AID protein expression was measured by Western, as shown in a representative blot. Quantification of AID protein was normalized to β-actin and bars indicate the average signal. P value, two-tailed equal variance Student's *t*-test. Both mRNA and protein data are from 3 experiments each using one mouse per genotype.

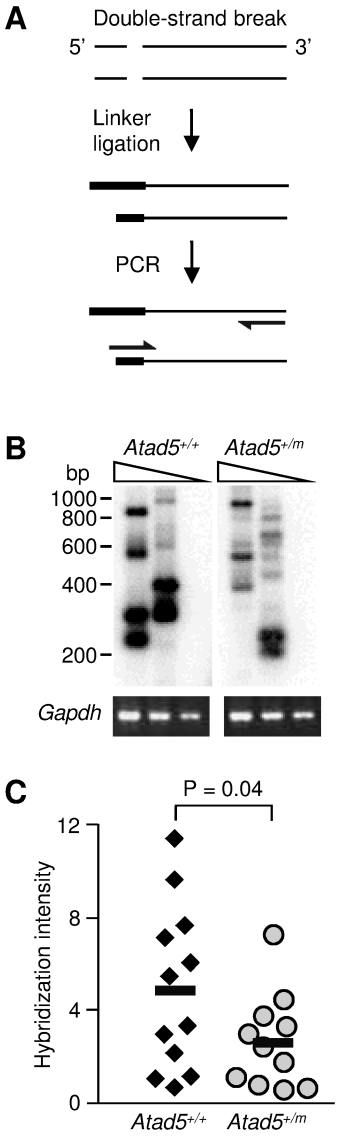

FIGURE 5.

LM-PCR assay to detect double-strand breaks. **(A)** Experimental design. A linker is ligated to break sites, and the DNA is amplified with primers (half-arrows) for the linker and S_{μ}. **(B)** Representative Southern blot with a probe specific for S_{μ}. LM-PCR was performed on 3-fold dilutions of DNA from cells stimulated for 2 days. Below, ethidium bromide staining for *Gapdh* (control for DNA input). **(C)** Quantification of breaks. Values were measured using the highest dilution of DNA and were calculated from 11 independent PCR reactions from 2 mice per genotype. Bars indicate the average signal. P value, one-tailed equal variance Student's *t*-test.

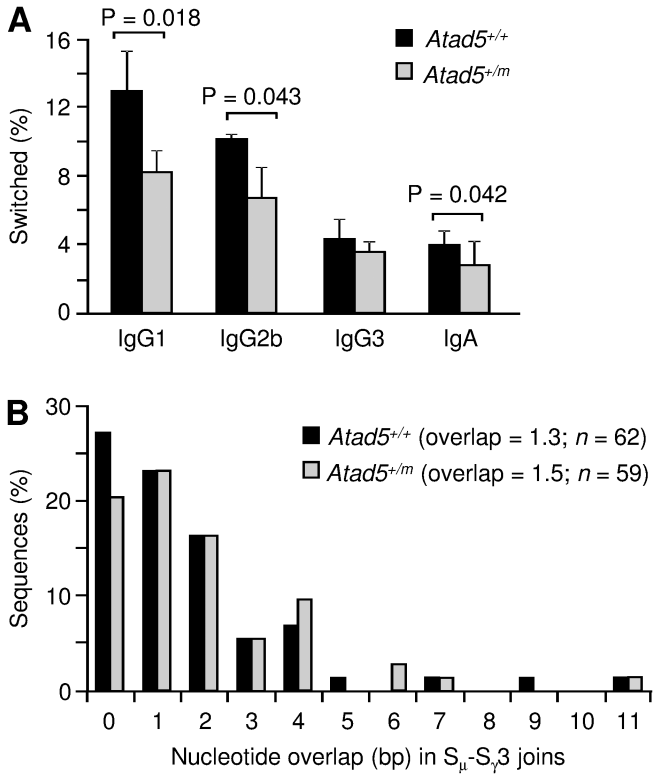

FIGURE 6.

CSR and microhomology at switch joins. **(A)** Percent of switched cells after 4 d stimulation. Error bars signify the SD of values from 3 independent experiments with one mouse per genotype per experiment. P value, two-tailed paired Student's *t*-test. **(B)** Microhomology in S_{μ}-$S_{\gamma}3$ switch joins from cells stimulated with LPS. Overlap lengths are shown on the x-axis. Mean overlap of identical bases is shown for *n* sequences from two independent experiments each using two mice per genotype.

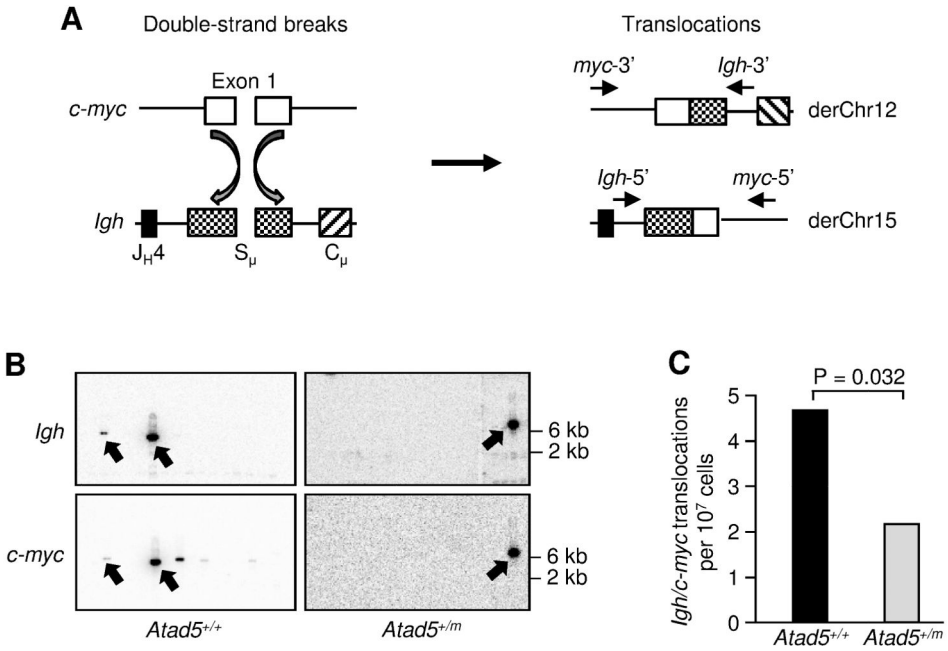

FIGURE 7.

Translocations between S_μ and *c-myc*. **(A)** Strategy to identify translocations. Double-strand breaks in exon 1(white box) of *c-myc* and the S_μ region (hatched box) of *Igh* lead to recombinations indicated by curved arrows. Translocations were detected using PCR primers (short arrows) for *Igh* or *c-myc*, as shown for both derivative chromosome 12 (derChr12) and derivative chromosome 15 (derChr15). **(B)** Representative Southern blots of derChr15 hybridized with either *Igh* or *c-myc* probes. Arrows depict bands that stained with both probes. **(C)** *Igh/c-myc* translocation frequencies per 10^7 cells on both derChr12 and derChr15. Cumulative values from 2 mice of each genotype with 368 $Atad5^{+/+}$ and 327 $Atad5^{+/m}$ amplifications. P value, two-tailed equal variance Student's *t*-test.